



Review

Photocatalytic degradation of organic dyes in the presence of nanostructured titanium dioxide: Influence of the chemical structure of dyes

A.R. Khataee^{a,*}, M.B. Kasiri^b^a Department of Applied Chemistry, Faculty of Chemistry, University of Tabriz, Tabriz, Iran^b Faculty of Applied Arts, Tabriz Islamic Art University, Tabriz, Iran

ARTICLE INFO

Article history:

Received 22 February 2010

Accepted 28 May 2010

Available online 8 June 2010

*Keywords:*TiO₂ nanomaterials

Photocatalysis

Dye structure

Advanced oxidation processes

Textile dye

ABSTRACT

Synthetic dyes are a major part of our life as they are found in the various products ranging from clothes to leather accessories to furniture. These carcinogenic compounds are the major constituents of the industrial effluents. Various approaches have been developed to remove organic dyes from the natural environment. Over the past few years, there has been an enormous amount of research with advanced oxidation processes (AOPs) as an effective method of wastewater treatment. Among AOPs, heterogeneous photocatalytic process using TiO₂ nanomaterials appears as the most emerging destructive technology due to its cost effectiveness and the catalyst inert nature and photostability. This review deals with the photocatalytic degradation of organic dyes containing different functionalities using TiO₂ nanomaterials in aqueous solution. It first discusses the photocatalytic properties of nanostructured TiO₂. The photocatalytic degradation rate strongly depends on the basic structure of the molecule and the nature of auxiliary groups attached to the aromatic nuclei of the dyes. So, this review then explains the influence of structure of dyes on their photocatalytic degradation rates. The influences of different substitutes such as alkyl side chains, methyl, nitrate, hydroxyl and carboxylic groups as well as the presence of chloro atom have been discussed in detail.

© 2010 Elsevier B.V. All rights reserved.

Contents

1. Introduction	9
2. Titanium dioxide nanomaterials: structural and photocatalytic properties	9
3. Photocatalytic removal of dyes by titanium dioxide nanomaterials	11
4. Influence of type of the dye on photocatalytic process efficiency	11
5. Influence of substitute of the dye on photocatalytic process efficiency	20
5.1. Influence of methyl group	20
5.2. Influence of nitrite group	24
5.3. Influence of alkyl side chains	24
5.4. Influence of chloro group	24
5.5. Influence of carboxylic group	24
5.6. Influence of sulfonic substituent	24
5.7. Influence of the number of hydroxyl groups	24
6. Conclusion	25
Acknowledgement	25
References	25

* Corresponding author. Tel.: +98 411 3393165; fax: +98 411 3340191.

E-mail addresses: a.khataee@tabrizu.ac.ir, ar.khataee@yahoo.com (A.R. Khataee), masoud.bagherzadeh-kasiri@uha.fr (M.B. Kasiri).

1. Introduction

Large amounts of dyes are annually produced and applied in different industries including textile, cosmetic, paper, leather, pharmaceutical and nutrition industries. There are more than 100,000 commercially available dyes with an estimation annual production of over 70,000 tons, 15% of which is lost during the dyeing process [1]. The presence of even trace concentration of dyes in effluent is highly visible and undesirable. It causes some serious problems to aquatic life and human health disorders [2]. These concerns have led to new and/or strict regulations concerning colored wastewater discharge as well as developing more efficient treatment technologies.

Various methods have been suggested to handle the dye removal from water such as biodegradation, coagulation, adsorption, advanced oxidation processes (AOPs) and the membrane process [3–8]. All these processes have some advantages or disadvantages over the other methods. A balanced approach is therefore needed to look into the worthiness on choosing an appropriate method which can be used to degrade the dye in solution.

Among the new methods of colorful wastewater treatment, AOPs based on the generation of very reactive species such as hydroxyl radicals have been proposed to oxidize quickly and none selectively a broad range of organic pollutants [9–11]. AOPs have been growing during the last decade since they are able to deal with the problem of dye destruction in aqueous systems. Among AOPs, heterogeneous photocatalysis using TiO_2 nanomaterials as photocatalyst appears as the most emerging destructive technology [12–17]. The key advantage of the photocatalytic process is its inherent destructive nature: it does not involve mass transfer; it can be carried out under ambient conditions (atmospheric oxygen is sufficient as oxidant) and may lead to complete mineralization of organic carbon into CO_2 . Moreover, nanostructured TiO_2 photocatalyst is largely available, inexpensive, non-toxic and shows relatively high chemical stability. Finally, TiO_2 photocatalytic process is receiving increasing attention because of its low cost when the sunlight is used as the source of irradiation [2,10].

The earliest description of photodecomposition of organic compounds and studies of effects of reaction parameters were reported by Kraeutler and Bard [18]. Heterogeneous photocatalysis has attracted constant research since its infancy considering the high number of excellent reviews and books devoted by many researchers [19,20].

Although photocatalytic degradation has broad generality for destruction of both organic and inorganic compounds, the focus of this review is on organic dyes. There are many studies dealing with the photocatalytic decolorization of specific textile dyes from different chemical categories, and most of them include a detailed examination of working conditions [21–27]. There are also some reviews concerning the mechanism and fundamentals of photocatalytic degradation of organic dyes [28–30]. On the contrary and to the best of our knowledge, there is not a review dealing with the influence of the structure of organic dyes on photocatalytic degradation efficiency in the presence of nanostructured titanium dioxide. The present review sheds light on the structure-degradability relation of the heterogeneous photocatalytic degradation of organic dyes and reports the effect of the dye chemical structure on the process efficiency.

2. Titanium dioxide nanomaterials: structural and photocatalytic properties

Titanium dioxide, C.I. No. 77891, also known as titanium(IV) oxide, CAS No. 13463-67-7 with molecular weight of 79.87 (g mol^{-1}) is the naturally occurring oxide of titanium with the

chemical formula TiO_2 . When used as a pigment, it is called “Titanium White” and “Pigment White 6”. Titanium dioxide is extracted from a variety of naturally occurring ores that contain ilmenite, rutile, anatase and leucosene, which are mined from deposits throughout the world. Most of titanium dioxide pigment in industry is produced from titanium mineral concentrates by the so-called chloride or sulfate process, either as rutile or anatase form. The primary Titanium White particles are typically between 200 and 300 nm in diameter, although larger aggregates and agglomerates are also formed [31].

Titanium dioxide (TiO_2) has a wide range of applications. It is used mostly as a pigment in paints, sunscreens, ointments, and toothpaste since its commercial production in the early twentieth century. Titanium dioxide pigments are inorganic chemical products used for imparting whiteness, brightness and opacity to a diverse range of applications and end-use markets, including coatings, plastics, paper and other industrial and consumer products. TiO_2 is considered a “quality-of-life” product with demand affected by gross domestic product in various regions of the world. TiO_2 as a pigment derives value from its whitening properties and opacifying ability (commonly referred to as hiding power). As a result of TiO_2 's high refractive index rating, it can provide more hiding power than any other commercially available white pigment. Commercial production of this pigment started in the early twentieth century during the investigation of ways to convert ilmenite to iron or titanium-iron alloys. The first industrial production of TiO_2 started in 1918 in Norway, the United States and Germany [31–34].

Crystals of titanium dioxide can exist in one of the three crystalline forms: rutile, anatase or brookite (Table 1). In their structures, the basic building block consists of a titanium atom surrounded by six oxygen atoms in a more or less distorted octahedral configuration. In all the three TiO_2 structures, the stacking of the octahedra results in threefold coordinated oxygen atoms.

The fundamental structural unit in these three TiO_2 crystals forms from TiO_6 octahedron units and has different modes of arrangement and links as presented in Fig. 1. In the rutile form, TiO_6 octahedra link by sharing an edge along the *c*-axis to form chains. These chains are then interlinked by sharing corner oxygen atoms to form a three-dimensional framework. Conversely in anatase, the three-dimensional framework is formed only by edge-shared bonding among TiO_6 octahedrons. It means that octahedra in anatase share four edges and are arranged in zigzag chains along. In brookite, the octahedra share both edges and corners, forming an orthorhombic structure [35–38].

In coming up with these crystal structures and to estimate the crystal grain size of anatase, rutile and brookite the X-ray diffraction (XRD) experimental method is used. Anatase peaks in X-ray diffraction are occurred at $\theta = 12.65^\circ$, 18.9° , and 24.054° , the rutile peaks are found at $\theta = 13.75^\circ$, 18.1° , and 27.2° while brookite peaks are encountered at $\theta = 12.65^\circ$, 12.85° , 15.4° , and 18.1° . θ represents the X-ray diffraction angle [39–41].

One of the important properties of the inorganic solid TiO_2 nanomaterials is its photocatalytic activity in many applications ranging from antibacterial surfaces to photocatalytic reactions. In addition to TiO_2 , there are a wide range of metal oxides and sulfides have been successfully tested in photocatalytic reactions [42,43]. They include ZnO [44], WO_3 [45], WS_2 [46], Fe_2O_3 [47], V_2O_5 [48], CeO_2 [49], CdS [50], and ZnS [51]. Interaction of these semiconductors with photons having an energy comparable (equal or higher) to the band gap may cause separating the conduction and the valence bands as illustrated in Fig. 2. This event is known as electron–hole pair generation. For TiO_2 , this energy can be supplied by photons with energy in the near ultraviolet range. This property promoted TiO_2 as a promising candidate in photocatalysis where solar light can be used as energy source [52]. In addition, TiO_2 nanomaterials are largely used as a photocatalyst owing to its beneficial charac-

Table 1
Crystallographic properties of rutile, anatase and brookite [35].

Crystal structure	Density (g/cm ³)	System	Space group	Cell parameters (nm)		
				a	b	c
Rutile	4240	Tetragonal	$D_{4h}^{14} - P4_2/mnm$	0.4584	–	0.2953
Anatase	3830	Tetragonal	$D_{2d}^{19} - I4_1/amd$	0.3758	–	0.9514
Brookite	4170	Rhombohedral	$D_{2h}^{16} - Pbca$	0.9166	0.5436	0.5135

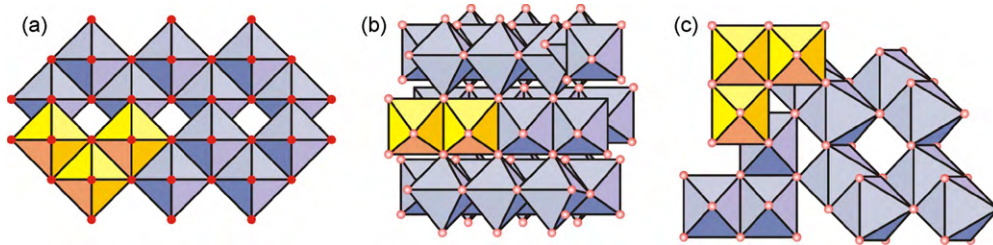
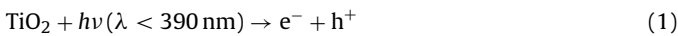


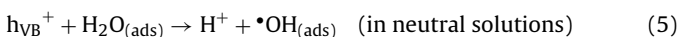
Fig. 1. Crystalline structure of: (A) anatase, (B) brookite and (C) rutile.

teristics which include high photocatalytic efficiency, physical and chemical stability, low cost and low toxicity.

As it can be observed from Fig. 2, when TiO₂ is illuminated with the light ($\lambda < 390$ nm), an electron excites out of its energy level and consequently leaves a hole in the valence band. Indeed, electrons are promoted from the valence band to the conduction band of TiO₂ to give electron–hole pairs (Eq. (1)) [43,53]:

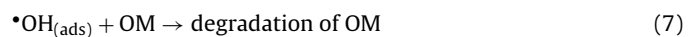
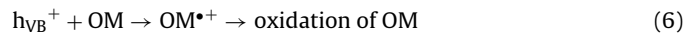


The valence band (h^+) potential is positive enough to generate hydroxyl radicals ($\bullet\text{OH}$) at the surface on TiO₂ and the conduction band (e^-) potential is negative enough to reduce molecular oxygen as shown in the following equations:



The hydroxyl radical is a powerful oxidizing agent which may attack the organic matters (OM) present at or near the surface of TiO₂. It is capable to degrade toxic and bioresistant compounds into harmless

species (e.g. CO₂, H₂O, etc.). This decomposition can be explained through the following reactions [53,54]:



In addition to the wide energy band gap, TiO₂ exhibits many other interesting properties, such as transparency to visible light, high refractive index and a low absorption coefficient. Anatase and rutile, the two principal polymorphs of TiO₂, are associated with energy band gap energies of 3.2 and 3.1 eV, respectively. It has been pointed out that the photodegradation reaction rate is much more rapid over anatase than in the case of rutile [55,56]. This reaction rate is mainly affected by the crystalline state and textural properties such as surface area and particle size of TiO₂ powder. However, these factors often vary in opposite ways, since a high degree of crystallinity is generally achieved through a high-temperature thermal treatment leading to a reduction in the surface area. Thus, optimal conditions for the synthesis TiO₂ nanomaterials have been sought to obtain materials of high photoactivity. Since photocatalytic reactions are generally studied in aqueous suspensions, problems arise from the formation of hard agglomerates through the diffusion of reactants and products as well as light absorption.

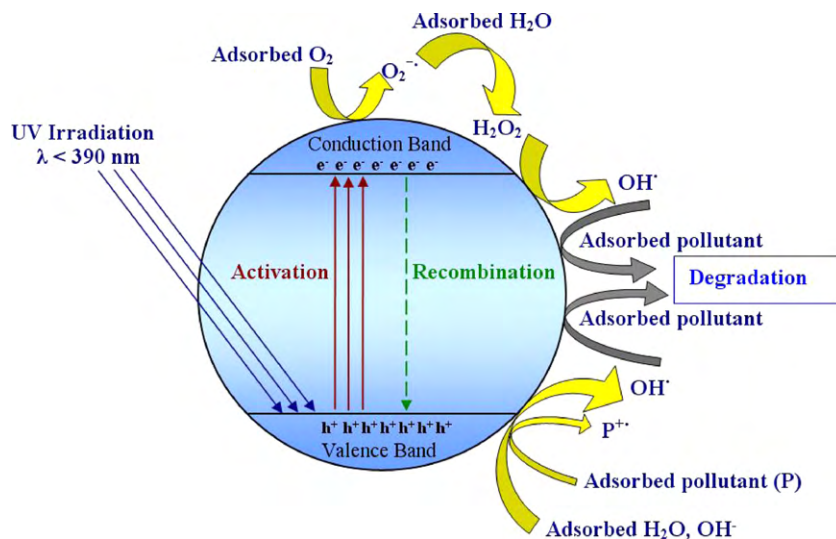


Fig. 2. General mechanism of the photocatalysis on TiO₂ nanomaterials.

The crystal structure of TiO₂ greatly affects its photocatalytic activity. Amorphous TiO₂ seldom displays photocatalytic activity due to the presence of nonbridging oxygen atoms in the bulk TiO₂, whose Ti–O atomic arrangement defects could act as the recombination centers of the photogenerated electron–hole pairs [52].

The photocatalytic performance of TiO₂ depends not only on its bulk energy band structure but also, to a large extent, on its surface properties. The larger the surface area per mass, the higher the photocatalytic activity. Decomposition of methylene blue over TiO₂ photocatalyst films indicates that the photocatalytic activity is strongly dependent on the film surface area of the photocatalyst. These films may have anatase crystal structure with different thicknesses and surface areas. They are prepared through the low-pressure metal-organic chemical vapor deposition (LPMOCVD) [57].

The type and density of surface states of TiO₂ nanomaterials are affected, among others, by the synthesis process. For instance, a soft mechanical treatment of TiO₂ nanopowder, for instance, was found to reduce significantly its photocatalytic activity in reduction of Cr(VI) [58]. On the other hand, treatment in either H₂ or N₂ plasma was found to enhance the activity within the visible-light range for certain reactions [59]. The interplay between processing conditions and photocatalytic activity remains largely a state-of-the-art and are beyond prediction at this point. Crystalline TiO₂ has typically been calcined or crystallized in oxidizing atmospheres, such as air and oxygen. The effect of the so-called inert atmospheres, such as N₂, Ar, and vacuum ($\sim 5 \times 10^3$ torr), has mostly been overlooked. It was found that the calcination atmosphere had significant effects on the photocatalytic activity of TiO₂ [60]. Calcination in either hydrogen or in vacuum results in a high density of defects and low surface hydroxyl coverage, thus yielding low activity. Calcination in Ar, in contrast, enhances visible-light excitation and high hydroxyl coverage, leading to higher activity [60].

TiO₂ nanomaterials are successfully used for the photocatalytic remediation of a variety of organic pollutants such as hydrocarbons, chlorinated hydrocarbons (e.g. CCl₄, CHCl₃, C₂HCl₃, phenols, chlorinated phenols, surfactants, pesticides, and organic dyes) as well as reductive deposition of heavy metals such as Pt⁴⁺, Pd²⁺, Au³⁺, Rh³⁺ and Cr³⁺ from aqueous solutions. TiO₂ nanomaterials have also been efficient in the destruction of biological materials such as bacteria, viruses and molds [61–65]. At the following sections, we present a detailed review of TiO₂ nanomaterials application for photocatalytic removal of a variety of organic dyes focusing in particular on structural effect of dyes on photocatalytic process.

3. Photocatalytic removal of dyes by titanium dioxide nanomaterials

A large amount of scientific articles have reported TiO₂-mediated photocatalytic degradation of organic dyes that Tables 2–6 summarize the results obtained.

Approximately 50–70% of the dyes available on the market are azo compounds followed by the anthraquinone group [66]. Some azo dyes and their dye precursors have been reported as human carcinogens [67–70]. Therefore azo dyes are pollutants of high environmental impact and were selected as the most relevant group of dyes concerning their degradation using TiO₂ assisted photocatalysis. Monoazo dyes were the major subject of the research in this field and Table 2 shows the structure and reactivity of studied dyes in the photocatalytic processes.

Azo dyes can be divided into monoazo, diazo and triazo classes according to the presence of one or more azo bonds (–N=N–). Azo dyes are found in various categories including acid, basic, direct, disperse, azoic and pigments. The structure and properties of diazo

and polyazo dyes that have been the subject of TiO₂-mediated photocatalysis researches are presented in Table 3.

Other groups of organic dyes including indigoid, anthraquinone, triarylmethane and xanthene dyes have also some serious environmental impacts. They have obtained the second rank in the photocatalytic process studies (see Tables 4–6). Generally, the sites near the chromophore (for instance, C–N=N– bond) is the attacked area in the photocatalytic degradation process. Photocatalytic destruction of the C–N= and –N=N– bonds leads to fading of the dyes.

According to the literature, both UV light and a photocatalyst, such as TiO₂ are needed for the effective destruction of organic dyes [26,39,43,44]. For instance, removal of Direct Red 23 by photocatalysis (UV/TiO₂) and photolysis (UV alone) processes was compared. In the presence of both TiO₂ and UV light, 54% of the dye was degraded at the irradiation time of 180 min. This was contrasted with ~2% degradation for the same experiment performed with photolysis process [53].

4. Influence of type of the dye on photocatalytic process efficiency

The chemical structure of the organic dyes has a considerable effect on the reactivity of these dyes on a TiO₂-mediated photodegradation system. This effect has been explored by different researchers. Neppolian et al. [74,111] have compared the photocatalytic degradation of three dyes (i.e. Reactive Yellow 17 (RY17), Reactive Red 2 (RR2) and Reactive Blue 4 (RB4)) in suspended and immobilized UV/TiO₂ systems. The energy source was sunlight and UV-C lamp (254 nm) and the photocatalyst type was TiO₂ obtained from Degussa P25 and Merck. The photocatalytic decolorization process was performed in different kinds of reactors including: UV source photocatalytic reactor, solar photocatalytic reactor and thin-film coated photocatalytic device. Chemical oxygen demand (COD) removal rate of RY17 was found to be higher than that of two other dyes, RR2 and RB4. The three dyes have well-defined absorption in both UV and visible region of the spectrum. In that respect the dyes are similar. The important structural difference among the three molecules is that in the case of RY17 and RR2 there is an azo group (–N=N–), which is not present in RB4 molecule (see Tables 2 and 4). This azo group is susceptible to photodegradation. That makes the first two dyes to degrade easily. Further –CH₂–OS₂– linkage in RY17 is also labile in the reaction environment. In RB4, the presence of anthraquinone structure and the absence of azo band make it resistant to photodegradation. These basic structural differences explain the observed order of the three dyes degradation (i.e. RY17 > RR2 > RB4).

In a similar work, Damodar et al. [94] have studied the degradation of three reactive dyes (i.e. Reactive Black 5, Reactive Blue 4 and Reactive Orange 16) by suspended and immobilized Solar/TiO₂ processes using TiO₂ pure anatase (BET = 15 m²/g) in thin-film surface reactor (see Tables 2–4). Their results showed that the removal of Reactive Orange 16 was maximum, closely followed by Reactive Blue 4. The removal of Reactive Black 5 was much less, particularly at higher concentrations. This may be attributed to several factors. First, it may be due to the difference in chemical structure of dyes, resulting in difference in adsorption characteristics and difference in susceptibility to photodegradation. The chemical structure of the dyes indicates that Reactive Black 5 has more complex structure, making it less photodegradable. Another reason may be due to absorption of light photon by dye itself leading to a less availability of photons for hydroxyl radical generation. It was observed from the absorption spectra of three dyes in near UV range that Reactive Black 5 strongly absorbs near UV radiation compared to Reactive Orange 16 and Reactive Blue 4, leading to less

Table 2
Structure and reactivity of monoazo dyes during the photocatalytic processes.

No	Color Index name and no.	Other name and acronym	Chemical structure	λ_{\max} (nm)	Mw (g/mol)	Photocatalytic process	Catalyst brand and size	Ref. no.
1	Acid Red 14 14720	Chromotrope FB AR14		515	502.43	UV/TiO ₂	P25 ^a	[43]
2	Reactive Red 2	Procion Red MX-5B MX-5B		538	615.33	UV/ZnO UV/TiO ₂	Merck 33 nm P25	[44] [71]
3	Acid Red 27 16185	Amaranth AR27		521	604.47	UV/TiO ₂	P25	[75]
4	Reactive Red 22 14824	RR22		511	590.00	TiO ₂ and Nafion-coated TiO ₂	P25	[76]

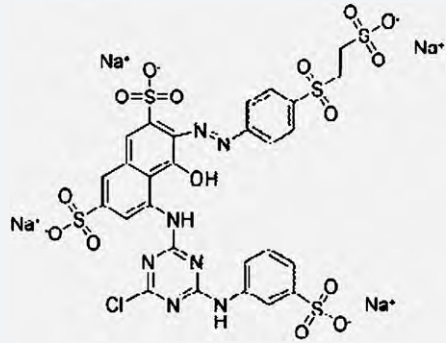
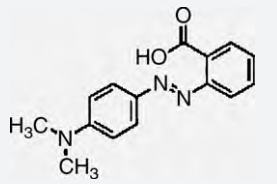
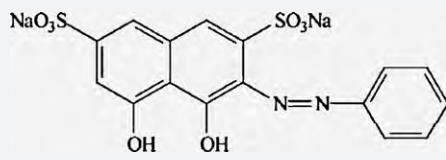
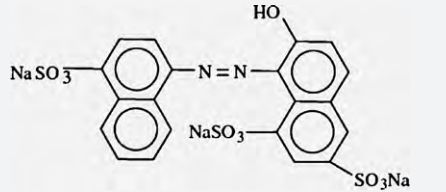
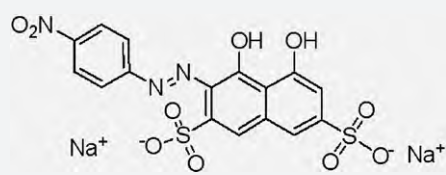
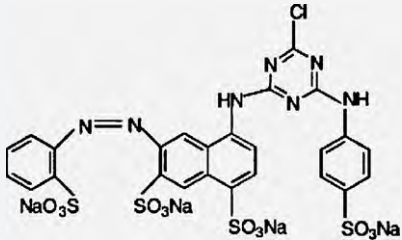
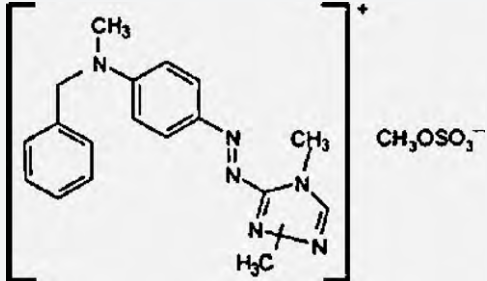
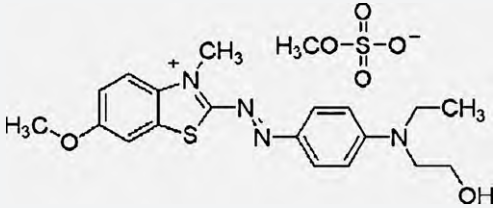
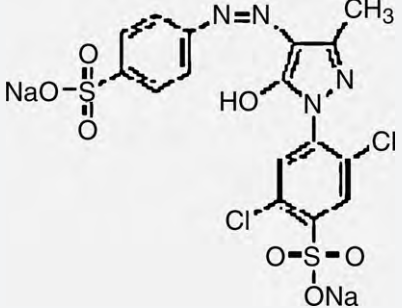
5	Reactive Red 198	RR198		518	968.21	UV/new TiO ₂ photocatalyst	P25	[77]
6	Acid Red 2 13020	Methyl Red MeRed		430	269.30	UV/TiO ₂	P25	[78]
						Immobilized TiO ₂ photoreactor	P25	[79]
						UV/silver ion doped TiO ₂	Merck 1 μm	[80]
7	Acid Red 29 16570	Chromotrope 2R AR29		510	468.37	UV/TiO ₂	P25	[83]
8	Acid Red 18 16255	New Coccine AR18		507	604.48	UV/TiO ₂	P25	[84]
							Fujititan TP-2 anatase	[85]
9	Acid Red 176 16575	Chromotrope 2B AR176		519	513.37	UV/TiO ₂	P25	[86]

Table 2 (Continued)

No	Color Index name and no.	Other name and acronym	Chemical structure	λ_{\max} (nm)	Mw (g/mol)	Photocatalytic process	Catalyst brand and size	Ref. no.
10	Reactive Red 15	Reactive Brilliant Red K-2G K-2G		500	807.00	UV/TiO ₂	P25	[73]
11	Basic Red 46	Maxilon Red GRL BR46		530	420.00	UV/TiO ₂	P25	[87]
12	Basic Blue 41 11105	BB41		600	482.57	Vis/TiO ₂	2–25 nm	[88]
13	Acid Yellow 17 18965	AY17		400	551.29	UV/TiO ₂	Fujititan TP-2 anatase	[85]

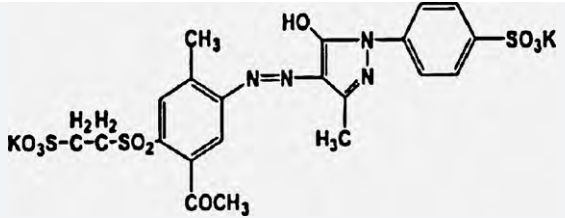
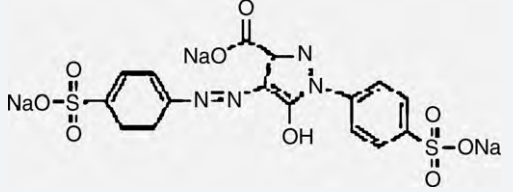
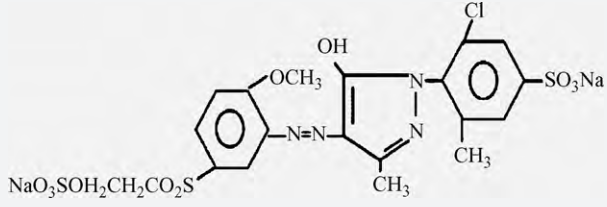
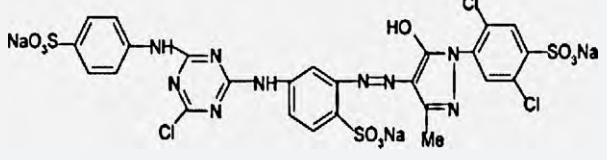
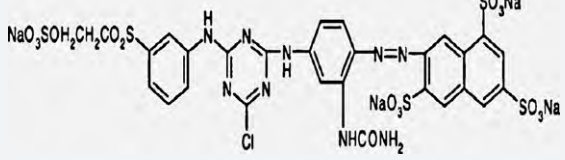

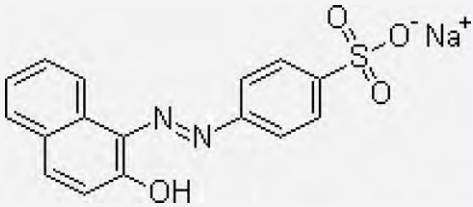
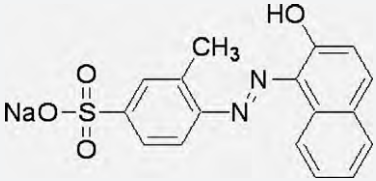
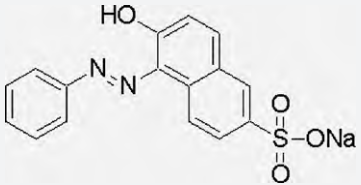
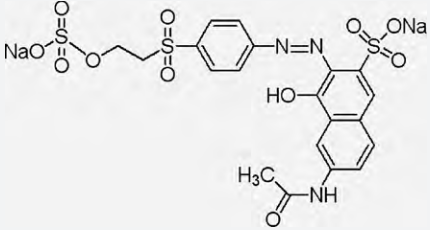
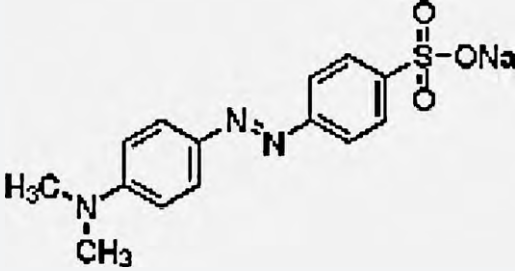
14	Reactive Yellow 17	Reactive Golden Yellow G RY17		426	682.17	Solar-UV/TiO ₂	P25	[74]
15	Acid Yellow 23 19140	Tartrazine Trat		455	534.36	UV/TiO ₂	Fujititan TP-2 anatase	[85]
16	Reactive Yellow 14	Remazol Yellow G RY14		410	669.00	UV/ZnO, TiO ₂ , CdS, Fe ₂ O ₃ and SnO ₂	TiO ₂ -P25, anatase ZnO 1–4 μm	[89]
17	Reactive Yellow 2	Light Yellow X6G		400	1110.00	UV/TiO ₂	Anatase 30 nm	[90]
18	Reactive Yellow 145	Reactive yellow 3RS RY145		419	1026.20	UV/TiO ₂	PC500 5–10 nm	[91]
19	Acid Orange 10 16230	Orange G, Wool Orange 2G OG		480	452.37	UV/TiO ₂ suspension	P25	[82]
					UV/TiO ₂ UV/immobilized TiO ₂	Fujititan TP-2 anatase Millennium PC-500	[85] [92]	

Table 2 (Continued)

No	Color Index name and no.	Other name and acronym	Chemical structure	λ_{\max} (nm)	Mw (g/mol)	Photocatalytic process	Catalyst brand and size	Ref. no.
20	Acid Orange 7 15510	Orange II A07		485	350.32	UV/TiO ₂	Fujititan TP-2 anatase	[85]
21	Acid Orange 8 15575	A08		490	364.35	UV/immobilized TiO ₂	Millennium PC-500	[92]
22	Acid Orange 12 15970	Crocein, Orange G		488	350.30	UV/immobilized TiO ₂	Millennium PC-500	[92]
23	Reactive Orange 16 17757	Remazol Brilliant, Orange 3R		494	617.54	Solar irradiation/TiO ₂	Anatase	[94]
24	Acid Orange 52 13025	Orange III, Methyl Orange MeOr			327.33	UV/TiO ₂ immobilized	Anatase	[81]

^a Degussa P25 (80% anatase, 20% rutile, particle size: 21 nm).

Table 3
Structure and reactivity of diazo and polyazo dyes during the photocatalytic processes.

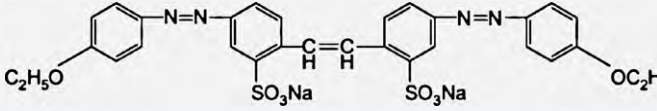
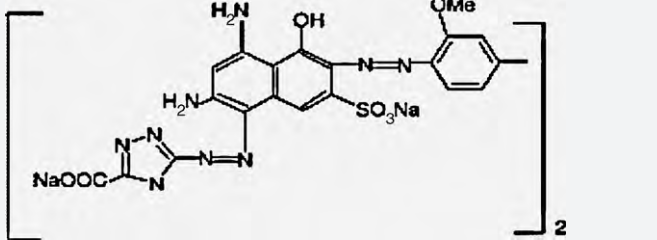
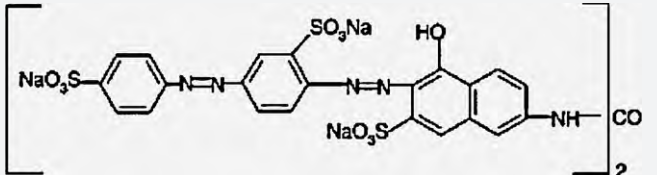
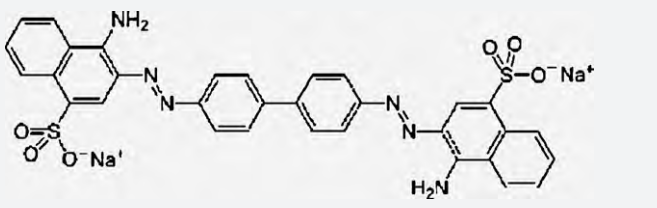
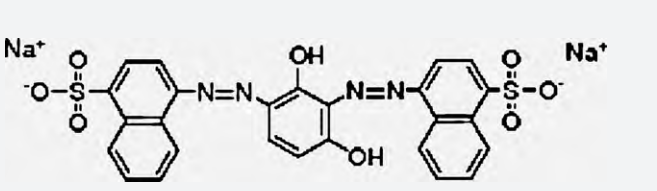
No.	Color Index name and no.	Other name and acronym	Chemical structure	λ_{\max} (nm)	Mw (g/mol)	Photocatalytic process	Catalyst brand and size	Ref. no.
1	Direct Yellow 12	Chrysophenine G		395.2	680.67	UV/TiO ₂	P25	[95]
2	Direct Blue 160	Copper Navy Blue RL		570	1373.00	UV/TiO ₂	Anatase 30 nm	[90]
3	Direct Red 80	Solophenyl red 3BL		530	872.50	UV/TiO ₂	Anatase 30 nm	[90]
4	Congo Red	Cobo Red CR		524	696.90	UV/TiO ₂ suspension	P25	[82]
5	Acid Brown 14	AB14		465	622.54	UV/TiO ₂ UV/ZnO	Fujititan TP-2 anatase P25 ZnO (Merck)	[85] [96]

Table 3 (Continued)

No.	Color Index name and no.	Other name and acronym	Chemical structure	λ_{\max} (nm)	Mw (g/mol)	Photocatalytic process	Catalyst brand and size	Ref. no.
6	Reactive Black 5 15510	Remazol Black B RB5		597	991.82	UV/TiO ₂	PC500 5–10 nm	[91]
7	Acid Black 1 20470	Naphtol blue black Amido black 10B		618	616.49	Solar irradiation/TiO ₂ H ₂ O ₂ /UV-C and TiO ₂ /UV-A	Anatase –	[94] [97]
						UV/TiO ₂	P25	[78]
						UV/TiO ₂	Fujititan TP-2 anatase	[85]
8	Direct Green 99	DG99		638	691.00	UV/TiO ₂	P25	[78]
						UV/new TiO ₂ photocatalyst	P25	[99]
						UV/SnO ₂ /TiO ₂	SnO ₂ ~5 and TiO ₂ ~30 nm	[98]

Table 4

Structure and reactivity of anthraquinone dyes during the photocatalytic processes.

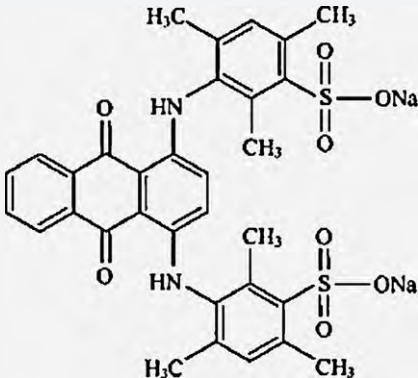
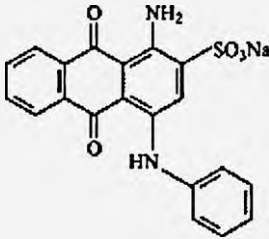
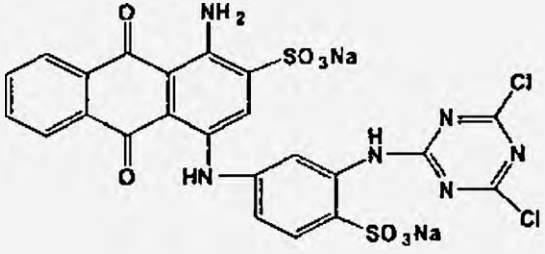
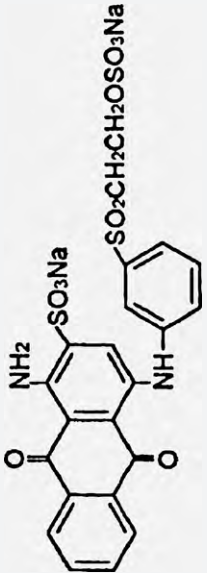
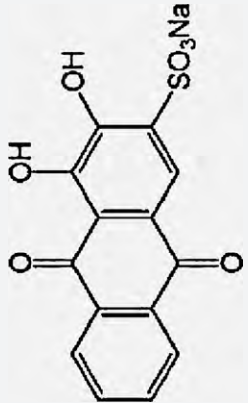
No.	Color Index name and no.	Other name and acronym	Chemical structure	λ_{\max} (nm)	Mw (g/mol)	Photocatalytic process	Catalyst brand and size	Ref. no.
1	Acid Blue 80 61585	AB80		626	678.68	UVA/TiO ₂ UV/TiO ₂	7.4 nm P25	[100] [101]
2	Acid Blue 25 62055	AB25		600	416.38	UV/TiO ₂	P25	[102]
3	Reactive Blue 4 61205	Procion blue MX-R RB4		596	637.43	Solar-UV/TiO ₂ Solar irradiation/TiO ₂	P25 Anatase	[74] [94]

Table 4 (Continued)

No.	Color index name and no.	Other name and acronym	Chemical structure	λ_{\max} (nm)	Mw (g/mol)	Photocatalytic process	Catalyst brand and size	Ref. no.
4	Reactive Blue 19 61200	Remazol Brilliant Blue R		592	626.54	UV/TiO ₂ UV/ZnO		[103]
5	Alizarin Red 58005	Alizarin Red S AR			342.26	UV/TiO ₂ suspension Vis/TiO ₂	P25 30–40 nm	[82] [104]

photodegradation.

Comparelli et al. [81] have studied the effect of two different substituents in photodegradation of two organic dyes (i.e. Methyl Red (MeRed) and Methyl Orange (MeOr)) in a batch UV/TiO₂ photoreactor with nanocrystal TiO₂ powders. TiO₂ nanoparticles (mean particle size: 6 nm) were deposited onto a quartz substrate irradiated with a medium pressure 200 W mercury lamp (emission >250 nm). Experiments taken under the best reaction conditions pointed out that the immobilized TiO₂ nanoparticles degraded MeRed more quickly than MeOr. This evidence suggests that a precise role must be played by the specific functional group, which differentiates the molecular structure of each dye (see Table 2). Probably, the adsorption of the target molecule on the immobilized TiO₂ nanoparticles surface should be regarded as a critical step toward efficient photocatalysis. MeRed adsorption through the carboxylic moiety can be reasonably expected to be weak especially at low pH, being mainly electrostatic in nature. As opposed, due to its favorable dimension and spatial geometry, the -SO₃⁻ attaches to surface Ti(IV) centers by assuming a bidentate coordination through the two sulfonic oxygens. This process would be accompanied by substitution of a surface coordinated -OH moieties. Because of the strong overlap between the 3d orbitals of the Ti(IV) atoms and the 2p orbitals of oxygens, the formation of Ti-O bonds would have a strong covalent character. As a result of MeOr complexation, a number of surface sites would be temporarily passivated, thus leading to catalyst deactivation and leaving the surface depleted in terminal -OH groups. This detrimental mechanism can remain operative over large periods of photocatalysis, as primary by-products of MeOr actually keep on bearing the sulfonic group.

5. Influence of substitute of the dye on photocatalytic process efficiency

5.1. Influence of methyl group

To find out the effect of methyl substituent on photocatalytic process efficiency, the decolorization of Acid Orange 7 (AO7) and Acid Orange 8 (AO8) could be a typical example. These two azo dyes have nearly the same structure (see Table 2); but the presence of -CH₃ group in AO8 molecular structure can slightly decrease the reactivity of this dye [74].

Khataee et al. [92] have studied the effect of molecular structure of three azo dyes (i.e. Acid Orange 10 (AO10), Acid Orange 12 (AO12) and Acid Orange 8 (AO8)) on photocatalytic degradation using immobilized TiO₂ nanoparticles (see Table 2). It was found that the photocatalytic decolorization kinetics of the dyes were in the order of AO10 > AO12 > AO8. Acid Orange 10, which has two sulfonic groups, exhibited a high adsorption yield, which can be attributed to both the high molecular weight of this molecule compared to the other dyes, and the additional sulfonic group. In AO10, due to its favorable dimension and spatial geometry, the -SO₃⁻ can attach to surface Ti(IV) centers by assuming a bidentate coordination through the two sulfonic oxygens. AO8 and AO12 have nearly the same structure; the presence of the alkyl group (-CH₃) in AO8 molecular structure can decrease slightly the adsorption of this dye. Hydroxyl radicals have a very short lifetime, so that they can only react where they are formed. Indeed, every group that tends to decrease the solubility of molecules in water will disfavor degradation. This explains, at least partly, why the adsorption efficiency of AO12 with a hydrophobic substituent clearly decreases. Another reason may be due to absorption of light photon by dye molecule itself leading to a less availability of photons for hydroxyl radical generation. AO8 strongly absorb near UV radiation compared to AO12 and AO10 leading to less photodegradation. The above-mentioned order (AO10 > AO12 > AO8) was observed in absorption spectra of the three dyes in UV range. The strong absorption of light

Table 5

Structure and reactivity of triarylmethane dyes during the photocatalytic processes.

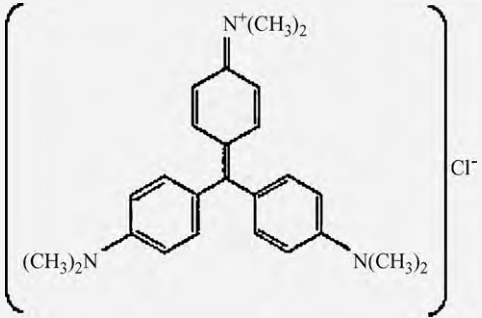
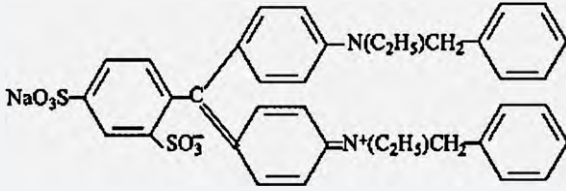
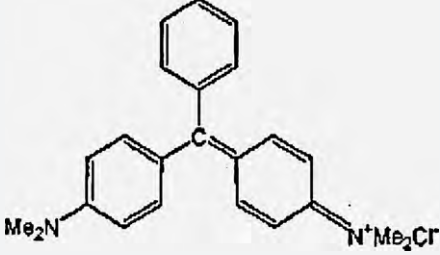
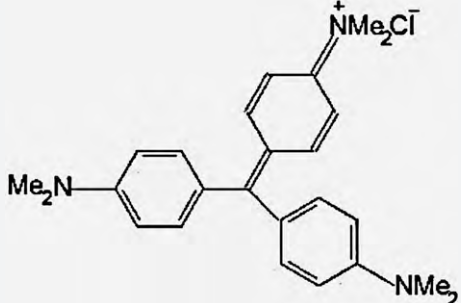
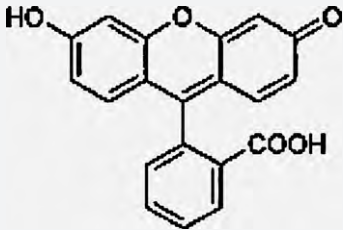
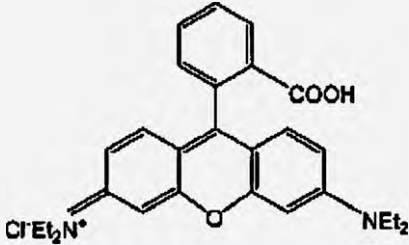
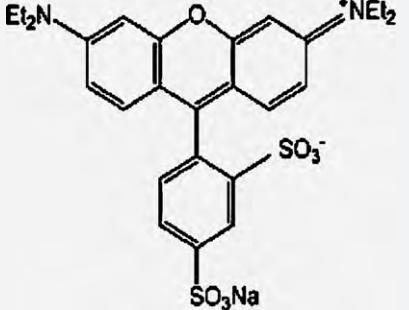
No.	Color Index name and no.	Other name and acronym	Chemical structure	λ_{max} (nm)	Mw (g/mol)	Photocatalytic process	Catalyst brand and size	Ref. no.
1	Basic Violet 3 42555	Crystal Violet CV		550	407.98	UV/silver ion doped TiO ₂ UV/ZnO	Merck 1 μm Merck	[80] [105]
2	Acid Blue 7	AB7		625	1168.00	UV/TiO ₂	P25	[78]
3	Malachite Green 42000	Basic Green 4 MG			364.91	Vis/TiO ₂	30–40 nm	[104]
4	Gentian Violet 42555 42535	Mixture of crystal violet and methyl violet		536		UV/TiO ₂	P25 PC500 (5–10 nm)	[106]

Table 5 (Continued)

No.	Color Index name and no.	Other name and acronym	Chemical structure	λ_{max} (nm)	Mw (g/mol)	Photocatalytic process	Catalyst brand and size	Ref. no.
5	Acid Blue 1 42045	Sulfan Blue Food Blue 3 Patent Blue VF		630	566.66	UV/TiO ₂	P25	[107]
6	Acid Blue 9 42090	Brilliant Blue FCF AB9		625	792.86	UV/TiO ₂ UV/synthesized TiO ₂	21 nm 6–11 nm	[10] [108]

Table 6
Structure and reactivity of xanthene dyes during the photocatalytic processes.

No.	Color Index name and no.	Other name and acronym	Chemical structure	λ_{\max} (nm)	Mw (g/mol)	Photocatalytic process	Catalyst brand and size	Ref. no.
1	Acid Yellow 73 45350	Fluorescein		490	332.00	Vis–UV/TiO ₂	TiO ₂ /SiO ₂ /γ-Fe ₂ O ₃ (TSF)	[109]
2	Rhodamine-B 45170	Basic Violet 10 Brilliant Pink B Rhodamine O		550	479.01	Vis/TiO ₂ Microwave/UV/TiO ₂	30–40 nm P25	[104] [110]
3	Sulforhodamine B 45100	Acid Red 52 SRB			580.65	Vis/TiO ₂	30–40 nm	[104]

by the dye molecules is thought to have an inhibitive effect on the photogeneration of holes or hydroxyl radicals, because of the lack of any direct contact between the photons and immobilized TiO₂. Indeed, it causes the dye molecules to adsorb light and the photons never reach the photocatalyst surface, thus the photodegradation efficiency decreases [92,112].

It is also important to notice that degradation pathway of organic dyes may be different. According to the proposal of Galindo and Kalt [113], only an addition of a •OH radical on an aromatic ring of molecules which do not contain a labile H atom (for instance Methyl Red) can occur. This mechanism is also unsatisfactory for hydroxy azo dyes (AO7 and AO8). In that case, abstraction of a H atom, carried by an oxygen atom in the azo form and by a nitrogen atom in the hydrazone form, competes with the addition of •OH radical on a phenyl or naphthyl nucleus [113].

5.2. Influence of nitrite group

In order to evaluate the influence of a nitrite group, the degradation of an analogous pair of dyes (i.e. Acid Red 29 (AR29) and Chromotrope 2B) can be mentioned (see Table 2). Chromotrope 2B contains a nitrite group in the para position with respect to the azo function. This substituent interacts with the phenyl ring and there is a consequent delocalization of the *p* electrons of the ring and of the unpaired electrons of the heteroatom. As a result, the phenyl ring is electron enriched, and the nitrite group thus favors attack of an electrophilic entity. The experiment confirms this hypothesis: Chromotrope 2B reaction rate is slightly higher than that of AR29 [83,86].

5.3. Influence of alkyl side chains

Hydroxyl radicals have a very short lifetime, so that they can only react where they are formed. Land and Ebert [114] indicated that its lifetime is, for instance, approximately 70 ns in the presence of 1 mM phenol. It means that using the Einstein–Smoluchowski equation ($\Delta x = (2Dt)^{1/2}$ with $D = 2.3 \times 10^{-5} \text{ cm}^2 \text{ s}^{-1}$ for •OH radicals) the inorganic radical can diffuse through an average distance of 180 Å. Thus oxidation reactions can only be successfully performed in homogeneous media. As it was previously mentioned, every group that tends to decrease the solubility of molecules in water will decrease the degradation process. This explains why the rate of decomposition clearly decreases with increasing length of the side chain, and consequently with increasing hydrophobicity of the dye molecule, as seen at the degradation of AB25 and RB19 [102,113]. A parallel reaction may take place between •OH radical and hydrogen atoms of the side chains. This reaction competes with destruction of the dye chromophore, without leading to a decrease in the absorbance of the solution.

5.4. Influence of chloro group

Considerable decrease of photocatalytic decolorization rate was observed when two or three chloro substituents were present on the phenyl ring of a pyrazolone dye. Indeed, comparison of Acid Yellow 17 (AY17) and Acid Yellow 23 (AY23) decolorization rates suggests that the difficulty of the dye to be degraded directly depends on the number of electron withdrawing chloro groups in the molecule. The decolorization kinetics of AY17 are less than those of AY23 [85].

The electron withdrawing inductive effect (–I effect) of chloro substituents largely surpasses the +M resonance effect (substituent is an electron releasing group), and consequently halogens deactivate the ring which carries them. Substitution of chloro groups in dye molecules by hydroxyl radicals may occur, leading to the formation of chloride anions in the solution. The degradation of

AY17 leads to colorless chlorinated compounds and removal of chloro atoms in the organic matter preferentially takes place with these organic products. This reaction is, however, going to compete with the dye chromophore destruction, because it also consumes hydroxyl radicals.

To compare the effect of different substituents on the process rate, Wang [115] has investigated the decolorization and mineralization of eight commercial dyes with different structures and different substitute groups containing chloro and sulfonic in a UV/TiO₂ suspension system (TiO₂; anatase, 9 m²/g). Total organic carbon (TOC), chloride and sulfate ions were measured during the process. Results indicate that the sulfonic-substituted dye is more reactive than the chloride-substituted dye in the photocatalytic process.

5.5. Influence of carboxylic group

To explore the effect of the presence of carboxylic substituent on photocatalytic decolorization rate, Lachheb et al. [82] have studied the decolorization of four organic dyes (i.e. Alizarin S, Crocein Orange G, Methyl Red and Congo Red) by UV/TiO₂ process. The applied photocatalyst was TiO₂ Degussa P25 (21 nm, 50 m²/g) and Millennium PC500 (5–10 nm, 320 m²/g). Photocatalyst was supported on a non-woven paper of synthetic fiber prepared by Ahlstrom firm. TiO₂ nanoparticles were also supported on glass plates using a sol–gel method. They compared photocatalytic decolorization efficiency of the dyes in the presence of immobilized TiO₂ nanoparticles in 1 l new cascade falling film photoreactor (called STEP). The photocatalytic rate constants were in the following order:

MethylRed(MR) > OrangeG(OG) ≈ AlizarinS(AS) > CongoRed(CR)

They have explained that the higher degradability of MR could be due to the presence of a carboxylic group which can easily react with H⁺ via a photo-Kolbe reaction. However, the presence of a withdrawing group such as –SO₃[–] is probably at the origin of the less efficient OG and AS degradations. Another suggestion to explain the different reactivity of these dyes could also be their ability to adsorption on TiO₂ surface [116].

5.6. Influence of sulfonic substituent

Surprisingly, the presence of the more powerful electron withdrawing sulfonic group on a molecule makes it only very slightly less sensitive to oxidation. Indeed, molecules with one, two or three sulfonic functions have almost the same reactivity with respect to oxidation by hydroxyl radicals. Acid Red 14 (AR14) containing two sulfonic groups is more reactive in a photocatalytic degradation process in comparison with Acid Red 18 (AR18) and Acid Red 27 (AR27) that contain three sulfonic substituents [69,75,84,85].

In fact, study of the influence of the sulfonic group is very difficult, because this substituent operates in different fields: it decreases electron density in the aromatic rings and the β nitrogen atom of the azo bond by –I and +M effects. On the other hand, it increases the hydrophilic–lipophilic balance of the dye molecules, and consequently slows down their aggregation degree [116,92].

5.7. Influence of the number of hydroxyl groups

The electronic properties of a hydroxyl group are –I and +M effects. That is why the photocatalytic decolorization rate of Acid Red 29 (containing two hydroxyl substituents) is more than that of Orange G (containing one hydroxyl substituent) [83,85]. In both dyes, one molecule contains a hydroxyl group next to the azo bond (see Table 2). But the resonance effect of a substituent operates

only when the group is directly connected to the unsaturated system. Therefore, to explain the effect of the hydroxyl group on the reactivity of the organic matter, only the field effect (–I) must be considered. The number of hydroxyl groups in the dye molecule can intensify this resonance and consequently, the degradation rate of the dye.

6. Conclusion

TiO₂-mediated photocatalytic processes have been widely used for degradation of organic dyes, due to the cost effectiveness and the catalyst inert nature and photostability. Photocatalytic process efficiency depends on different parameters, particularly on the type and surface status of TiO₂, the chemical structure of the dyes and the nature of functional groups attached on the dye molecule. This review focuses on the influence of the chemical structure of organic dyes on photocatalytic degradation efficiency in the presence of TiO₂ nanomaterials. Photocatalytic degradation rate of monoazo dyes is higher than that of dyes with anthraquinone structure. The presence of methyl and chloro groups in the dye molecule decreases slightly the process efficiency while a nitrite group acts in an opposite direction. Alkyl side chain decreases the solubility of molecule in water and consequently disfavors the photocatalytic degradation process. The dyes containing more sulfonic substituents are less reactive in the photocatalytic process, while hydroxyl group intensifies the electron resonance in the molecule and the degradation rate of the dye.

Photocatalytic degradation takes place at the surface of the catalyst. Dye molecules adsorb onto the surface of TiO₂ by electrostatic attraction and get mineralized by non-selective hydroxyl radicals. Therefore, the adsorption of the target molecule on TiO₂ surface may be regarded as a critical step toward efficient photocatalysis.

Acknowledgement

The authors thank the University of Tabriz, Iran for financial supports.

References

- [1] H. Zollinger, *Color Chemistry: Synthesis Properties and Application of Organic Dyes and Pigments*, VCH Publishers, New York, 1987.
- [2] R. Pourata, A.R. Khataee, S. Aber, N. Daneshvar, *Desalination* 249 (2009) 301–307.
- [3] N. Daneshvar, A.R. Khataee, M.H. Rasoulifard, M. Pourhassan, *J. Hazard. Mater.* 143 (2007) 214–219.
- [4] N. Daneshvar, H. Ashassi Sorkhabi, M.B. Kasiri, *J. Hazard. Mater.* 112 (2004) 55–62.
- [5] N. Daneshvar, S. Aber, A. Khani, A.R. Khataee, *J. Hazard. Mater.* 144 (2007) 47–51.
- [6] N. Daneshvar, M. Ayazloo, A.R. Khataee, M. Pourhassan, *Bioresour. Technol.* 98 (2007) 1176–1182.
- [7] A. Aleboye, M.B. Kasiri, M.E. Olya, H. Aleboye, *Dyes Pigments* 77 (2008) 288–294.
- [8] M.B. Kasiri, H. Aleboye, A. Aleboye, *Appl. Catal. B* 84 (2008) 9–15.
- [9] T. Sano, E. Puzenat, C. Guillard, C. Geantet, S. Matsuzawa, *J. Mol. Catal. A: Chem.* 284 (2008) 127–133.
- [10] A.R. Khataee, V. Vatanpour, A.R. Amani, *J. Hazard. Mater.* 161 (2009) 1225–1233.
- [11] M. Kitano, M. Matsuoka, M. Ueshima, M. Anpo, *Appl. Catal. A* 325 (2007) 1–14.
- [12] G. Liu, T. Wu, J. Zhao, H. Hidaka, N. Serpone, *Environ. Sci. Technol.* 33 (1999) 2081–2087.
- [13] J. Zhao, T. Wu, K. Wu, K. Oikawa, H. Hidaka, N. Serpone, *Environ. Sci. Technol.* 32 (1998) 2394–2400.
- [14] M.R. Hoffmann, S.T. Martin, W. Choi, D.W. Bahnemann, *Chem. Rev.* 95 (1995) 69–96.
- [15] I.K. Konstantinou, T.A. Albanis, *Appl. Catal. B* 42 (2003) 319–335.
- [16] A.L. Linsebigler, L. Guangquan, J.T. Yates, *Chem. Rev.* 95 (1995) 735–758.
- [17] G. Burgeth, H. Kisch, *Coord. Chem. Rev.* 230 (2002) 40–47.
- [18] B. Kraeutler, A.J. Bard, *J. Am. Chem. Soc.* 100 (1978) 5985–5992.
- [19] S. Kwon, M. Fan, A.T. Cooper, H. Yang, *Crit. Rev. Environ. Sci. Technol.* 38 (2008) 197–226.
- [20] F. Ibney Hai, K. Yamamoto, K. Fukushi, *Crit. Rev. Environ. Sci. Technol.* 37 (2007) 315–377.
- [21] N. Daneshvar, D. Salari, A. Niaei, A.R. Khataee, *J. Environ. Sci. Health B* 41 (2006) 1273–1290.
- [22] U.L. Gaya, A.H. Abdullah, *J. Photochem. Photobiol. C: Photochem. Rev.* 9 (2008) 1–12.
- [23] F. Meng, Z. Sun, *Mater. Chem. Phys.* 118 (2009) 349–353.
- [24] A. Fujishima, T.N. Rao, D.A. Tryk, *J. Photochem. Photobiol. C: Photochem. Rev.* 1 (2000) 1–20.
- [25] A. Fujishima, X. Zhang, C. R. Chim. 9 (2006) 750–760.
- [26] N. Daneshvar, M.J. Hejazi, B. Rangarany, A.R. Khataee, *J. Environ. Sci. Health B* 39 (2004) 285–296.
- [27] K. Pirkanniemi, M. Sillanpaa, *Chemosphere* 48 (2002) 1047–1060.
- [28] U.G. Akpan, B.H. Hameed, *J. Hazard. Mater.* 170 (2009) 520–529.
- [29] I.K. Konstantinou, T.A. Albanis, *Appl. Catal. B* 49 (2004) 1–14.
- [30] M.A. Rauf, S. Salman Ashraf, *Chem. Eng. J.* 151 (2009) 10–18.
- [31] Kirk-Othmer, *Encyclopedia of Chemical Technology*, vol. 19, fourth edition, Wiley-Interscience Publication, 1996.
- [32] H. Takeda, O. Ishitani, *Coord. Chem. Rev.* 254 (2010) 346–354.
- [33] R. Zallen, M.P. Moret, *Solid State Commun.* 137 (2006) 154–157.
- [34] X. Chen, *Chin. J. Catal.* 30 (2009) 839–851.
- [35] U. Diebold, *Surf. Sci. Rep.* 48 (2003) 53–229.
- [36] Y. Li, T.J. White, S.H. Lim, *J. Solid State Chem.* 177 (2004) 1372–1381.
- [37] M. Yan, F. Chen, J. Zhang, M. Anpo, *J. Phys. Chem. B* 109 (2005) 8673–8678.
- [38] R. Janisch, P. Gopal, N. Spalding, *J. Phys.: Condens. Matter* 17 (2005) 657–689.
- [39] N. Daneshvar, M.H. Rasoulifard, F. Hosseinzadeh, A.R. Khataee, *J. Hazard. Mater.* 143 (2007) 95–101.
- [40] M.P. Moret, R. Zallen, D.P. Vijay, S.B. Desu, *Thin Solid Films* 366 (2000) 8–10.
- [41] G.A. Mansoori, T.R. Bastami, A. Ahmadvan, Z. Eshaghi, *Annu. Rev. Nano Res.* 2 (2008) 439–494.
- [42] A. Mills, S. Le Hunte, *J. Photochem. Photobiol. A* 108 (1997) 1–35.
- [43] N. Daneshvar, D. Salari, A.R. Khataee, *J. Photochem. Photobiol. A* 157 (2003) 111–116.
- [44] N. Daneshvar, D. Salari, A.R. Khataee, *J. Photochem. Photobiol. A* 162 (2004) 317–322.
- [45] X.F. Cheng, W.H. Leng, D.P. Liu, J.Q. Zhang, C.N. Cao, *Chemosphere* 68 (2007) 1976–1984.
- [46] D. Jing, L. Guo, *Catal. Commun.* 8 (2007) 795–799.
- [47] J. Bandara, U. Klehm, J. Kiwi, *Appl. Catal. B* 76 (2007) 73–81.
- [48] K. Teramura, T. Tanaka, M. Kani, T. Hosokawa, T. Funabiki, *J. Mol. Catal. A: Chem.* 208 (2004) 299–305.
- [49] Y. Zhai, S. Zhang, H. Pang, *Mater. Lett.* 61 (2007) 1863–1866.
- [50] K.G. Kanade, B. Jin-Ook, U.P. Mulik, D.P. Amalnerkar, B.B. Kale, *Mater. Res. Bull.* 41 (2006) 2219–2225.
- [51] C.L. Torres-Martínez, R. Kho, O.I. Mian, R.K. Mehra, *J. Colloid Interface Sci.* 240 (2001) 525–532.
- [52] R. Richards, *Surface and Nanomolecular Catalysis*, CRC Press/Taylor & Francis Group, 2006.
- [53] N. Daneshvar, D. Salari, A. Niaei, M.H. Rasoulifard, A.R. Khataee, *J. Environ. Sci. Health A* 40 (2005) 1605–1617.
- [54] M.A. Behnajady, N. Modirshahla, *Photochem. Photobiol. Sci.* 5 (2006) 1078–1081.
- [55] V. Loddò, G. Marcò, C. Martò, L. Palmisano, V. Rives, A. Sciafania, *Appl. Catal. B* 20 (1999) 29–45.
- [56] S. Bakardjieva, J. Subrt, V. Stengl, M. Dianez, M. Sayagues, *Appl. Catal. B* 58 (2005) 193–202.
- [57] S. Jung, S. Kim, N. Imaishi, Y. Cho, *Appl. Catal. B* 55 (2005) 253–257.
- [58] K. Madhusudan Reddy, D. Guin, S.V. Manorama, A.R. Reddy, *J. Mater. Res.* 19 (2004) 2567–2575.
- [59] M. Nakamura, N. Negishi, S. Kutsuna, T. Ihara, S. Sugihara, K. Takeuchi, *J. Mol. Catal. A: Chem.* 161 (2000) 205–212.
- [60] N.L. Wu, M.S. Lee, Z.J. Pon, J.Z. Hsu, *J. Photochem. Photobiol. A* 163 (2004) 277–280.
- [61] X. Wang, J.C. Yu, P. Liu, X. Wang, W. Sua, X. Fua, *J. Photochem. Photobiol. A* 179 (2006) 339–347.
- [62] M. Zheng, M. Gu, Y. Jin, G. Jin, *Mater. Sci. Eng. B* 77 (2000) 55–59.
- [63] K. Tennakone, K.G.U. Wijayantha, *J. Photochem. Photobiol. A* 113 (1998) 89–92.
- [64] M.N. Pons, A. Alinsafi, F. Evenou, E.M. Abdulkarim, O. Zahraa, A. Benhammou, A. Yaacoubi, A. Nejmeddine, *Dyes Pigments* 74 (2007) 439–445.
- [65] N. Keller, G. Rebmann, E. Barraud, O. Zahraa, V. Keller, *Catal. Today* 101 (2005) 323–329.
- [66] P.C. Vandevivere, R. Bianchi, W. Verstraete, *J. Chem. Technol. Biotechnol.* 72 (1998) 289–302.
- [67] C. Gomes da Silva, J.L. Faria, *J. Photochem. Photobiol. A* 155 (2003) 133–143.
- [68] M.A. Brown, S.C. De Vito, *Crit. Rev. Environ. Sci. Technol.* 23 (1993) 249–324.
- [69] F. Zhang, A. Yediler, X. Liang, *Chemosphere* 67 (2007) 712–717.
- [70] M. Işık, D.T. Sponza, *J. Hazard. Mater.* 114 (2004) 29–39.
- [71] C. Hu, J.C. Yu, Z. Hao, P.K. Wong, *Appl. Catal. B* 46 (2003) 35–47.
- [72] H. Jin, Q. Wu, W. Panga, *J. Hazard. Mater.* 141 (2007) 123–128.
- [73] C. Hu, J.C. Yu, Z. Hao, P.K. Wong, *Appl. Catal. B* 42 (2003) 47–55.
- [74] B. Neppolian, H.C. Choi, S. Sakthivel, B. Arabindoo, V. Murugesan, *J. Hazard. Mater.* 89 (2002) 303–317.
- [75] M.A. Behnajady, N. Modirshahla, N. Daneshvar, M. Rabbani, *Chem. Eng. J.* 127 (2007) 167–176.
- [76] W.Y. Wang, Y. Ku, *Colloids Surf. A* 302 (2007) 261–268.
- [77] S. Kaur, V. Singh, *J. Hazard. Mater.* 141 (2007) 230–236.

- [78] B. Zielinska, J. Grzechulska, R.J. Kalenczuk, A.W. Morawski, *Appl. Catal. B* 45 (2003) 293–300.
- [79] N.M. Mahmoodi, M. Arami, N. Yousefi Limaee, *J. Hazard. Mater.* 133 (2006) 113–118.
- [80] A.K. Gupta, A. Pal, C. Sahoo, *Dyes Pigments* 69 (2006) 224–232.
- [81] R. Comparelli, E. Fanizzaa, M.L. Curri, P.D. Cozzoli, G. Mascolo, R. Passino, A. Agostiano, *Appl. Catal. B* 55 (2005) 81–91.
- [82] H. Lachheb, E. Puzenat, A. Houas, M. Ksibi, E. Elaloui, C. Guillard, J.M. Herrmann, *Appl. Catal. B* 39 (2002) 75–90.
- [83] M. Qamar, M. Saquib, M. Muneer, *Desalination* 186 (2005) 255–271.
- [84] S. Mozia, M. Tomaszewska, A.W. Morawski, *Desalination* 185 (2005) 449–456.
- [85] K. Tanaka, K. Padermpole, T. Hisanaga, *Water Res.* 34 (2000) 327–333.
- [86] M. Qamar, M. Saquib, M. Muneer, *Dyes Pigments* 65 (2005) 1–9.
- [87] A.R. Khataee, *Environ. Technol.* 30 (2009) 1155–1168.
- [88] E. Stathatos, T. Petrova, P. Lianos, *Langmuir* 17 (2001) 5025–5030.
- [89] M. Muruganandham, N. Shobana, M. Swaminathan, *J. Mol. Catal. A: Chem.* 246 (2006) 154–161.
- [90] M.H. Habibi, A. Hassanzadeh, S. Mahdavi, *J. Photochem. Photobiol. A* 172 (2005) 89–96.
- [91] A. Aguedach, S. Brosillon, J. Morvan, E. Lhadi, *Appl. Catal. B* 57 (2005) 55–62.
- [92] A.R. Khataee, M.N. Pons, O. Zahraa, *J. Hazard. Mater.* 168 (2009) 451–457.
- [93] K. Venkata Subba Raa, A. Rachela, M. Subrahmanyamb, P. Boule, *Appl. Catal. B* 46 (2003) 77–85.
- [94] R.A. Damodar, K. Jagannathan, T. Swaminathan, *Sol. Energy* 81 (2007) 1–7.
- [95] A.P. Toor, A. Verma, C.K. Jotshi, P.K. Bajpai, V. Singh, *Dyes Pigments* 68 (2006) 53–60.
- [96] S. Sakthivel, B. Neppolian, M.V. Shankar, B. Arabindoo, M. Palanichamy, V. Murugesan, *Sol. Energy Mater. Sol. Cells* 77 (2003) 65–82.
- [97] I.A. Alaton, I.A. Balcioglu, *J. Photochem. Photobiol. A* 141 (2001) 247–254.
- [98] K. Vinodgopal, I. Bedja, P.V. Kamat, *Chem. Mater.* 8 (1996) 2180–2187.
- [99] B. Wawrzyniak, A.W. Morawski, *Appl. Catal. B* 62 (2006) 150–158.
- [100] C.H. Ao, M.K.H. Leung, R.C.W. Lam, D.Y.C. Leung, L.L.P. Vrijmoed, W.C. Yam, S.P. Ng, *Chem. Eng. J.* 129 (2007) 153–159.
- [101] A.B. Prevot, C. Baiocchi, M.C. Brussino, E. Pramauro, P. Savarino, V. Augugliaro, G. Marci, L. Palmisano, *Environ. Sci. Technol.* 35 (2001) 971–976.
- [102] I. Bouzaida, C.J. Ferronato, M. Chovelon, M.E. Rammah, J.M. Herrmann, *J. Photochem. Photobiol. A* 168 (2004) 23–30.
- [103] C.A.K. Gouvêa, F. Wypych, S.G. Moraes, N. Durán, N. Nagata, P. Peralta-Zamora, *Chemosphere* 40 (2000) 433–440.
- [104] J. Yang, C. Chen, H. Ji, W. Ma, J. Zhao, *J. Phys. Chem. B* 109 (2005) 21900–21907.
- [105] S. Rodríguez Couto, A. Domínguez, A. Sanromán, *Chemosphere* 46 (2002) 83–86.
- [106] M. Saquib, M. Muneer, *Dyes Pigments* 56 (2003) 37–49.
- [107] C. Chen, C. Lu, F. Mai, C. Weng, *J. Hazard. Mater.* 137 (2006) 1600–1607.
- [108] A.R. Khataee, H. Aleboye, A. Aleboye, *J. Exp. Nanosci.* 4 (2009) 121–137.
- [109] F. Chen, Y. Xie, J. Zhao, G. Lu, *Chemosphere* 44 (2001) 1159–1168.
- [110] S. Horikoshi, H. Hidaka, *Environ. Sci. Technol.* 36 (2002) 1357–1366.
- [111] B. Neppolian, H.C. Choi, S. Sakthivel, B. Arabindoo, V. Murugesan, *Chemosphere* 46 (2002) 1173–1181.
- [112] N. Daneshvar, A. Aleboye, A.R. Khataee, *Chemosphere* 59 (2005) 761–767.
- [113] C. Galindo, A. Kalt, *Dyes Pigments* 42 (1999) 199–207.
- [114] E.J. Land, M. Ebert, *Trans. Faraday Soc.* 63 (1967) 1181–1190.
- [115] Y. Wang, *Water Res.* 34 (2000) 990–994.
- [116] C. Guillard, H. Lachheb, A. Houas, M. Ksibi, E. Elaloui, J.M. Herrmann, *J. Photochem. Photobiol. A* 158 (2003) 27–36.